3. Anatomy of recently active convergent plate interface zones – structures and processes within a subduction channel

3.1. General remarks

Here, we present concepts of plate interface structures and processes which are obtained by geophysical methods, numerical modeling and sandbox simulations, in order to compare them with the studied structures and processes of fossil convergent plate margins.

3.2. Concepts of plate interface processes

Cloos and Shreve (1988 a, b) have introduced the subduction channel concept denoting a zone between the upper and the lower plate of convergent plate margins (Fig. 3.1). This zone may typically be up to a few kilometers wide, and probably extends to a depth of more than 100 km (Gerya and Stöckhert 2002). During convergent plate motion material transport is performed within the subduction channel by conveying incoming sediments from the oceanic plate and slivers of oceanic and/or continental material down into the mantle, and by forced return-flow of low-viscosity material back to shallow crustal levels or even to the surface (Ábalos et al. 2003, Gerya et al. 2002). The material within the subduction channel exhibits a velocity gradient towards both plates (Fig. 3.1) (Gerya and Stöckhert 2002) – the material within the subduction channel has neither overcome the velocity of the overriding plate nor has it reached the velocity of the incoming plate. Material is partly scraped off and may either be accreted to the front of the accretionary wedge (frontal accretion) or to the base of the hanging wall (basal accretion) leading to duplex formation and antiformal stacking (e.g. von Huene and Scholl 1991). Material may also be removed from the tip (frontal tectonic erosion) or the base (basal tectonic erosion) of the upper plate by tectonic erosion (e.g. Clift and Vannucchi 2004). Both accretion and tectonic erosion cause a shift of the currently active subduction thrust. Therefore, Beaumont et al. (1999) refined the existing model of Cloos and Shreve (1988a, b) by defining the area above the subduction channel and below the hanging wall as a subduction conduit, in which material is slowly accumulated by tectonic underplating or removed by tectonic erosion. Consequently, we assume a fluctuating thickness of the subduction channel in space and time, and the active subduction megathrust is not a stationary feature, but composed of transiently active interfaces within and at the boundaries of the subduction channel.

Subduction channels developing at erosive margins should be composed of deformed slope sediments, continental basement and cover-rocks in addition to the pelagic and hemipelagic sediments of accretive subduction channels. Strain localization in subduction channels may preserve original sedimentary and magmatic textures in blocks of all sizes. These blocks are bounded by a network of active shear zones or sheared matrix (Ábalos et al. 2003) that promote the downward transport of incoming material. The deformational record of a subduction channel is persistently renewed due to continuous processes such as sediment subduction and tectonic erosion. Only when material finally left the active parts of the subduction channel and became accreted to the base of the hanging wall, the deformational record can be preserved. Deformation of the material leaving the subduction channel during accretion to the base of the upper plate is caused by permanent strain accumulation due to the velocity gradient between material flow within the channel and the upper plate.

Long-term deformation within a subduction channel is assumed to be

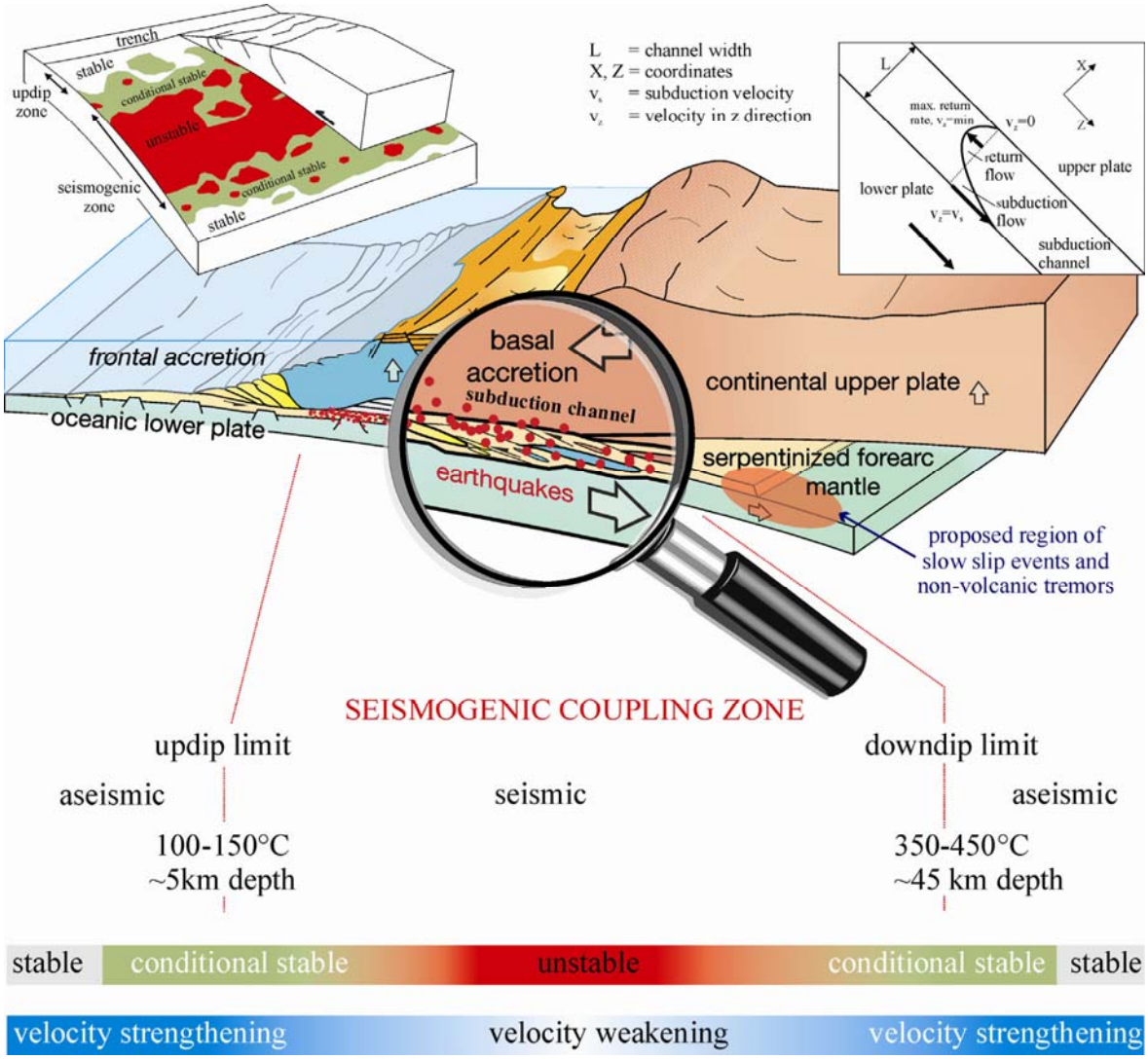

Figure 3.1: Schematic profile of a convergent plate margin with its subduction channel and the seismogenic coupling zone. The subduction channel may be defined by gradients in the flow velocity of the deforming material with respect to the upper and the lower plate (right inset, modified after Gerya and Stöckhert 2002). The updip limit of seismogenic coupling (about 5 km) is probably caused by the dehydration of stable sliding smectite to unstable sliding illite or chlorite (Hyndman et al. 1997). The downdip limit, i.e. the maximum depth of thrust earthquakes and aftershocks (Peacock and Hyndman 1999), is located at approx. 45 km, and may be caused by the increasing dominance of ductile behavior (Nedimović et al. 2003, Oleskevich et al. 1999) or the serpentinization of the forearc mantle leading to a talc rich layer, which lubricates the plate interface (Hyndman et al. 1997, Peacock and Hyndman 1999). Model of frictional conditions (left inset) modified and extended downdip following Bilek and Lay (2002) delineating stable areas, conditionally stable and unstable regions. These areas are variable in space and time. Seismic slip (i.e. velocity weakening behavior) cannot occur in stable areas, which are characterized by a velocity strengthening behavior of the involved material. Earthquakes only nucleate within unstable regions, but they can also propagate into the conditionally stable field (see text for detail).

mainly characterized by stable sliding. However, at a shorter time scale, unstable slip occurs in the upper part of the subduction channel within a limited depth range along the plate interface, i.e. a depth of 5 km to 45 km (Fig. 3.1, so-called seismogenic coupling zone, e.g. Ruff and Kanamori 1983, Tichelaar and Ruff 1993), causing major interplate earthquakes. The exact location of earthquake nucleation and the succeeding distribution of slip are mainly constrained by asperities or the

variation of the material state, which control the strength of the otherwise weak subduction channel (Pacheco et al. 1993, Ruff 1999).

According to conceptual models, the updip limit of the seismogenic coupling zone is probably caused by the dehydration of stable sliding smectite to unstable sliding illite or chlorite, or due to the interaction of the subduction channel with a rigid backstop (upper plate basement [Hyndman et al. 1997]). However, Saffer and Marone (2003) reported a velocity-strengthening behavior of illite in laboratory experiments, which contradicts to its proposed seismic behavior. Therefore, they suggest other temperature- and depth-dependent processes, such as cementation, consolidation and slip localization to be important for changing the frictional behavior of subduction zone material (see also e.g. Sobolev et al. 2006). Additionally, the alignment of clay minerals due to shearing is a key factor controlling the strength and frictional behavior of clay-rich gouges (Saffer and Marone 2003). The proposed processes take place over a broad range of pressure and temperature conditions. Therefore, Wang and Hu (2006) state that the updip limit of seismogenic behavior must be a transitional feature.

The downdip limit, i.e. the maximum depth of thrust earthquakes and aftershocks (Peacock and Hyndman 1999), is located at approx. 45 km (Fig. 3.1), and may be caused by increasing ductile behavior of the deformed material (Nedimović et al. 2003, Oleskevich et al. 1999). Another discussed process is the serpentinization of the forearc mantle leading to a talc rich layer along the contact of both plates, which lubricates the plate interface (Hyndman et al. 1997, Peacock and Hyndman 1999). Fluids necessary for this proposed serpentinization are thought to be provided by prograde metamorphism of the subducted slab (oceanic plate and metamorphosed remnants of its sedimentary cover).

Scholz (1998) described different stability regimes along the plate interface (Fig. 3.1): stable, unstable, and conditional stable. The stable regime exhibits velocity strengthening behavior, the unstable regime velocity weakening. Conditional stability defines a region, which exhibits a stable regime under quasistatic conditions. Such areas are thought to be variable in space and time (Schwartz and Rokosky 2007, and references therein). According to Bilek and Lay (1998, 1999) seismic slip cannot occur in the stable zone, because elastic strain is relaxed by aseismic creep. Earthquakes only nucleate within unstable regions, but they can also propagate into conditionally stable areas (Scholz 1998, Moore and Saffer 2001). The distribution of stable, unstable and conditional stable regions may be heterogeneous both downdip and along strike the plate interface producing islands of locked asperities embedded in weaker sedimentary material due to the heterogeneous distribution of subducted material, and the continuously occurring processes along the plate interface (e.g. cementation, dehydration) (Fig. 3.1).

3.3. Material input and fluid release

The material transported into subduction zones consists of clay minerals, carbonates and trench-filling sand (Hashimoto et al. 2006). Therefore, not only the transition from smectite to illite should play an important role in controlling the interface properties, but also the deformational behavior of sandstone blocks or layers should be taken into account. Downward transported sediments strongly influence the physical properties of the plate interface, because they are less rigid than the rest of the subducting plate. Diverse sediment input will lead to spatiotemporal modifications of the physical properties

along the plate interface (i.e. frictional regimes). Bilek and Lay (1998, 1999) assumed that subducted sediments increase in rigidity and frictional resistance due to compaction, and are therefore responsible for unstable slip, and for the decrease of source durations in earthquake rupturing. Scholz (1998) reported a velocity strengthening behavior for less consolidated sediments, possibly promoting areas of stable sliding. Compaction and phase transitions within both sediments and the subducting slab lead to dewatering and dehydration, providing fluids to the plate interface system. This water release increases the pore pressure, and therefore reduces effective stress and effective friction. This in turn increases the probability of fracture formation. Further down the plate interface loss of fluids increases the strength of the sediments. The replacement of clay minerals by zeolite or quartz enforces velocity weakening due to the velocity weakening behavior of low-porosity rocks and framework silicates (Moore and Saffer 2001), thus increasing the probability of earthquakes. Whether this change is abrupt or gradual is mostly defined by the general permeability along the plate interface.

Fluids play an important role within the subduction system. They influence metamorphic reactions, and they are thought to be responsible for the generation of seismicity due to their influence on the effective normal stresses acting on a fault plane. When the fluid pressure is close to the lithostatic pressure, the probability of earthquake occurrence increases. Then, the rupture decreases the fluid pressure to hydrostatic levels due to dilatancy and higher fault connectivity. In this stage the probability of further earthquakes is decreased (Renard et al. 2000). According to Husen and Kissling (2001) the accumulation of high stresses along the plate interface and the thereby caused fabric development leads to a sealing of the plate interface zone, which contributes to the trapping of fluids, and the thereby caused increase in fluid pressure (hydrostatic fluid pressure above the seal, lithostatic fluid pressure below the seal; see also Chapter 4.8.4.). Only major earthquakes might be able to break the seal, and allowing fluids to migrate upwards due to the gradient in fluid pressure. Therefore, the amount of water entering the system is crucial for the mechanical properties of the subduction zone interface.

The very low coefficient of friction in the order of 0.25 to 0.08 (Byrne and Fischer 1990) along the plate interface might result from high fluid pressure or material with a low frictional strength. Fluid overpressure will facilitate the development of tensile fractures, such as described by Hashimoto et al. (2006) in sandstone blocks from a tectonic mélange of the Shimanto Belt, Japan.

Most of the water is bounded in the incoming sediments or within fracture zones of the downgoing oceanic plate. According to Iwamori (1998) the oceanic crust contains about 6 wt-% water in chlorite, lawsonite and amphibole. This amount is reduced to less than 3 wt-% at 50 km depth. Pore water of the incoming sediments will be expelled at shallow depth < 10 km, and bound water is released in the temperature range between 80°C to 150°C due to the transformation of opal to quartz, and clay minerals to mica (Moore and Saffer 2001, Peacock 2000). Between 100°C and 150°C there is a peak in hydrocarbon production (Selley 1998), where solid organic matter is transferred into fluids. This fluid generation potential ends at ~150°C (Moore and Saffer 2001). Due to the porosity collapse in basalt at 300°C to 500°C, most of its pore water will be expelled or the water might contribute to reactions of high temperature minerals into low temperature minerals such as zeolites, which afterwards starts to dehydrate. Hyndman and Peacock (2003)

pointed out, that water release and water consumption by the growth of hydrous minerals are two competing processes. According to Peacock (2000) most of the water which is liberated > 10 km depth should originate from altered basalts or gabbros of the subducting oceanic plate.

Another important process associated with fluid flow is the serpentinization of the forearc mantle. Fluids required for this process might be released from the downgoing slab, allowing the hydration of the complete forearc mantle over tens of millions of years (Hyndman and Peacock 2003). The fluid flow is assumed to be fracture controlled rather than pervasive (Hyndman and Peacock 2003).

3.4. Earthquake distribution

Convergent plate boundaries at continental margins belong to the tectonically most active areas on earth and are endangered by devastating earthquakes. To get information about their spatiotemporal distribution is crucial in improving hazard assessments.

Seismicity at convergent plate margins is distributed within several geotectonic positions, and subdivided into intraplate and interplate earthquakes. Intraplate earthquakes nucleate within the subducting slab (e.g. outer-rise events, events within the Wadati-Benioff zone) or within the back-arc region of the overriding plate. Interplate seismicity at convergent plate margins is concentrated only within a narrow zone in the uppermost part of the subduction channel, i.e. a depth range between ~5 km to ~45 km depth (seismogenic zone). This interplate seismicity is responsible for the largest earthquakes ever recorded (e.g. Chile 1960 M_W 9.5, Alaska 1964 M_W 9.2, Ruff 1996). To better understand its implications for the studied fossil counterparts, we examined the spatial and temporal distribution of interplate seismicity based on data gained from the NEIC and Harvard catalogs, and from the combined CINCA ’95 and Task Force network. The data were kindly provided by Dietrich Lange (University of Potsdam) and Monika Sobiesiak (GFZ Potsdam), respectively.

In general, interplate earthquakes are distributed along the plate interface zone forming a narrow belt (in a 2D view) up to a few kilometers wide, which depends on the quality in relocation of the single seismic events. They cluster within the subduction channel and the basal parts of the upper plate, and are more diffuse distributed towards greater depths (Figs. 3.2, 3.3, 3.4). Consequently, interplate earthquakes clearly image the subduction plate interface zone.

Additionally, we used seismic data for aftershocks (295 events) from the 1995 Antofagasta earthquake (Northern Chile) in order to analyze a limited time window within the seismic cycle. We carefully evaluated the aftershock sequence by examining the different categories of aftershock focal mechanisms to study the spatiotemporal distribution of recent seismicity at a currently active subduction zone (Figs. 3.4, 3.5). The last big event in northern Chile occurred in 1995 near Antofagasta. This M_W 8.0 event ruptured the subduction interface 180 km along strike with an average slip of about 5 m in the depth interval between 10 km and 50 km. Despite the well defined plate interface the width of the zone of seismic activity defined by the aftershocks corresponds to about 3 km. The main shock was a thrust event, but the succeeding events, which occurred along the seismogenic coupling zone during the narrow time span of the recorded aftershocks (2 month) show all possible kinds of focal mechanisms (thrust faults, normal faults, and strike-slip faults) (Fig. 3.5). This has one critical implication for field-based structural analyses: It makes it

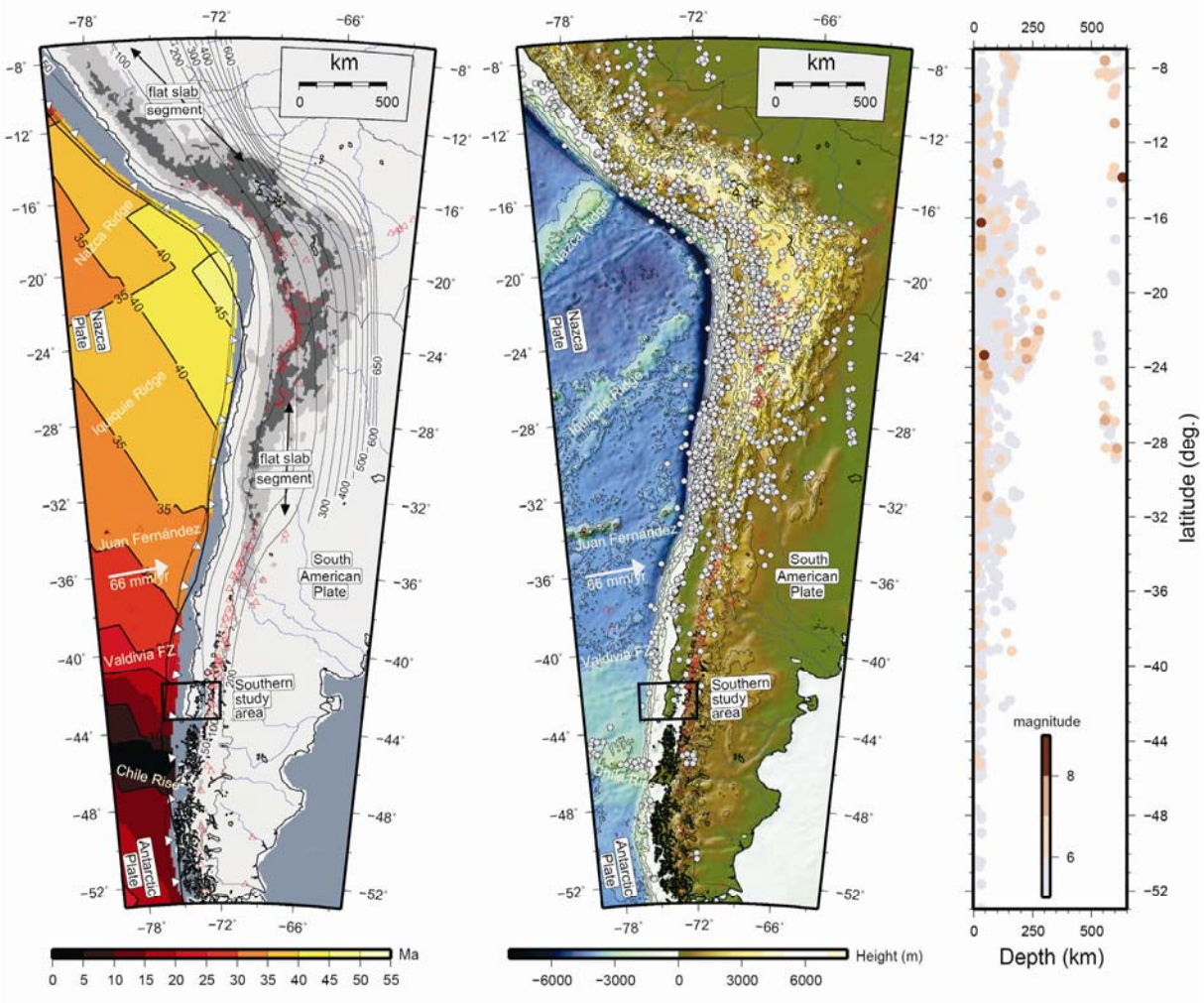

Figure 3.2: Overview of the central and southern Andes between 7°S and 53°S including seafloor ages (Müller et al. 1997), contours of the top of the subducting Nazca plate (Gudmundsson and Sambridge 1998) (left part). Grey dots represent seismicity gained from the NEIC catalog (middle part). The right part shows the seismicity distribution with depth, color coded by magnitude. Note there is a strong clustering of earthquakes within the uppermost part of the plate interface zone. Modified after Lange (2007).

difficult to use fault plane data gained from outcrops of first-order fault zones in order to obtain a relative event chronology on the basis of their kinematics.

We embedded all aftershocks by plotting their spatial distribution in 3D. This resulted in an undulating surface ("earthquake surface", Fig. 3.6) that indicates a broad area of seismic activity within the depth range of the seismogenic coupling zone outlined by the occurrence of the aftershocks, rather than a single sharp subduction thrust fault being active during the recorded time interval.

The slip accompanying earthquakes accounts only for a part of the total plate tectonic displacement (e.g. Schwartz and Rokosky 2007). In recent times, several studies start to concentrate on other strain releasing processes, such as slow slip events and associated non-volcanic tremors (e.g. Obara 2002, Rogers and Dragert 2003, Brown et al. 2005). However, their physical mechanisms remain questionable. Slow slip events (or silent earthquakes) are thought to be related with fluid migration on or nearby the plate interface, tremors may result from shear failure during slow slip (for an overview see Schwartz and Rokosky 2007). Most of the slow slip

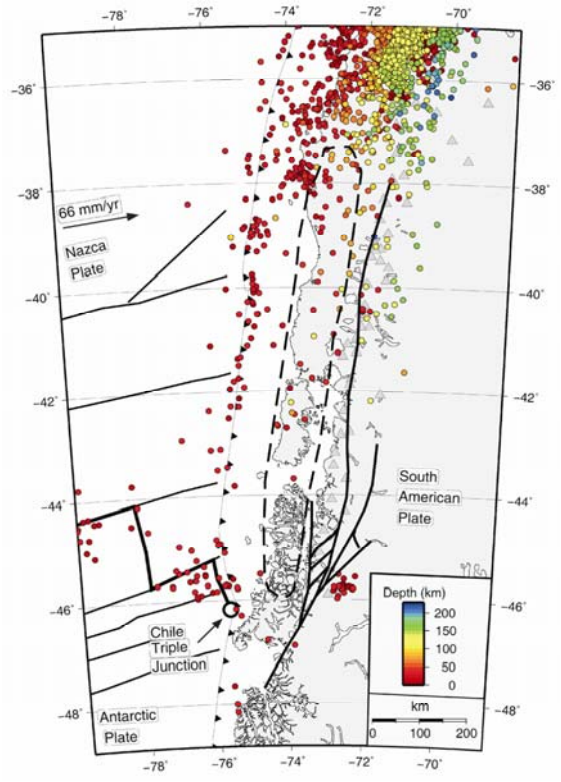

Figure 3.3: Seismicity distribution color coded with depth for Southern Chile based on the NEIC catalog for events between 1990 to 2007. Note there is a strong clustering of earthquakes within the uppermost part of the plate interface zone. Downdip the plate interface there is a more diffuse distribution of seismicity. Modified after Lange (2007).

events occur downdip the seismogenic zone in the transitional or stable sliding region. However, their exact position remains unclear. One of the objectives for this and for future field-based studies is to find possible field expression of ancient slow slip events and associated tremors (see Chapter 4.8.3.).

3.5. Geophysical signatures

Seismic reflection and refraction data provide further constraints for the structure of convergent plate margins. The active and passive seismic experiments conducted at the convergent Chile margin ANCORP (Oncken et al. 1999), SPOC (Krawczyk et al. 2003), and TIPTEQ (e.g. Micksch et al. 2006) provide the first complete high resolution coverage of the entire seismogenic zone of the plate interface (Fig. 3.7). Thereby, the downgoing plate depicts a sharp reflector due to its impedance contrast to the overlying upper plate. In addition, along the southern Chile margin the upper plate is highly reflective showing slightly upward convex continuous reflection bands (see also Fig. 1.6). They are interpreted to represent an ancient accretionary wedge (Krawczyk et al. 2003, Glodny et al. 2005). In general, the reflectivity of the plate interface zone increases to a certain depth and subsequently decreases downdip. According to the ANCORP working group (Oncken et al. 1999), this reduction in reflectivity starts at about 80 km depth, maybe caused by dehydration reactions and eclogitization of the subducting oceanic slab. These proposed processes increase the density of the subducted material, and therefore reduce the impedance contrast to the overlying material, and consequently the ability to resolve structures (Oncken et al. 1999, Krawczyk et al. 2003). Furthermore, along Vancouver Island, Nedimović et al. (2003) reported a transition from a single sharp reflector to a broad zone of reflectivity with varying thickness downdip the plate interface zone in the lower stable sliding region of the plate interface. According to these authors, this reflectivity zone is structurally interpreted as interlayered mafic and/or sedimentary rocks or fluids trapped within intensively sheared sedimentary rocks. A non-structural interpretation refers the reflectivity zone to thin dipping lenses of high porosity (Hyndman 1988). Also Krawczyk et al. (2003) interpreted such reflective elements along the Chilean subduction zone as trapped fluids.

According to Calvert et al. (2003) intense shearing and therewith associated structures (i.e. foliation) are responsible for seismic reflectivity. Therefore, Nedimovic et al. (2003) interpret the broad reflectivity

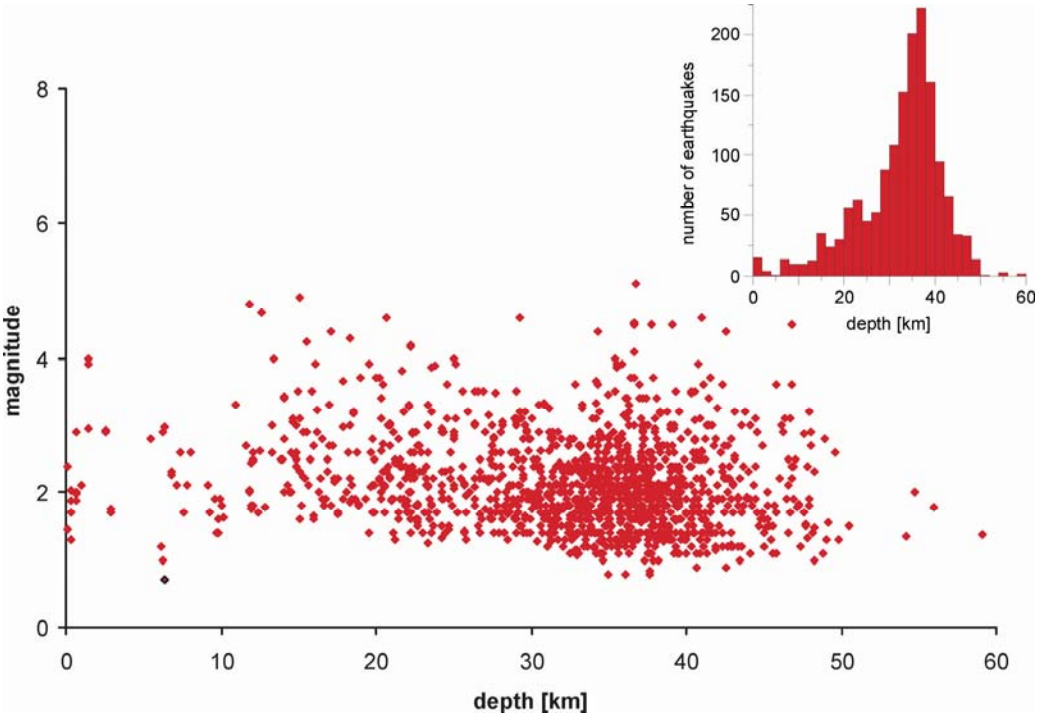

Figure 3.4: Magnitude-frequency-depth distribution for the 1995 Antofagasta aftershock sequence. The majority of the aftershocks occurs in the depth range of the seismogenic coupling zone (see inset of historgram). Data source based on the combined CINCA´95 and Task Force network (e.g. Sobiesiak 2000).

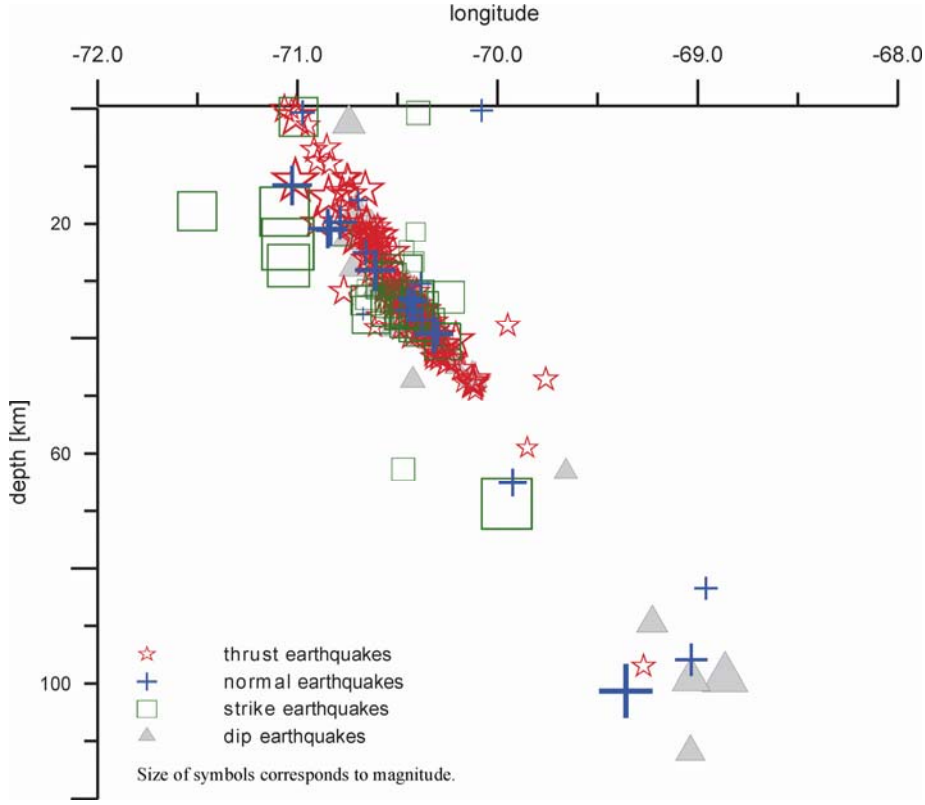

Figure 3.5: Distribution of different focal mechanisms for the 1995 Antofagasta aftershock sequence. There is no preferred appearance of one group of fault plane solutions (thrust faults, normal faults, and strike slip faults) following the main shock event (thrust fault). In contradiction, all possible kinds of focal mechanisms occur along the seismogenic coupling zone during the narrow time span of the recorded aftershocks. This makes it difficult to use fault plane data gained from outcrops of first-order fault zones in order to obtain a relative event chronology on the basis of their kinematics. Data source as above.

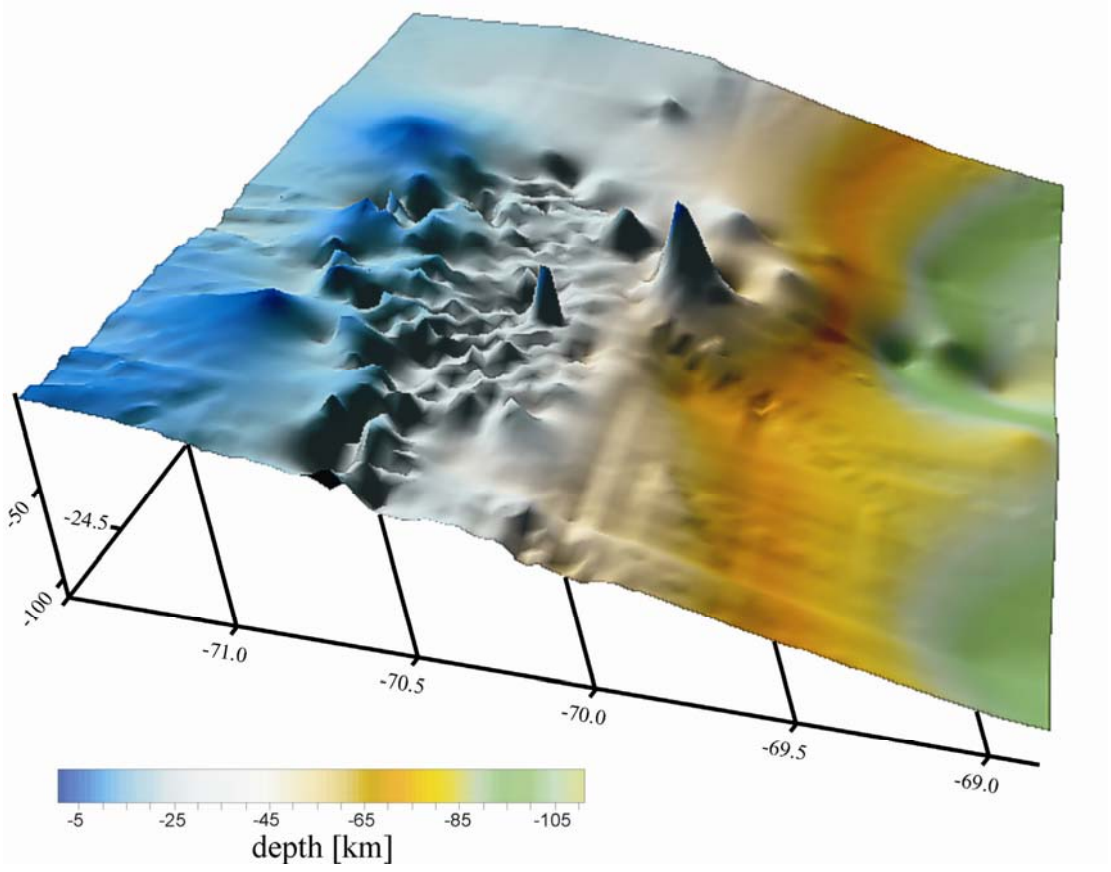

Figure 3.6: Reconstruction of the "earthquake surface" for the 1995 Antofagasta subduction earthquake aftershock sequence. Consider, the undulating surface indicates a broader area of seismic activity within the depth range of the seismogenic coupling zone rather than a single sharp subduction thrust fault being active during recorded aftershocks. Data source based on the combined CINCA´95 and Task Force network (e.g. Sobiesiak 2000).

band downdip the plate interface to be caused by mylonitic rocks, which have been formed where the temperature exceeds the 250°C to 350°C isotherms, and ductile behavior starts to dominate. Consequently, the reflectivity band observable along the plate interface could be the result of both trapped fluids and shearing (see also Chapter 4).

According to Krawczyk et al. (2003, 2006), the assumed subduction channel along the Chile margin is located between the sharp reflector of the downgoing oceanic plate and the highly reflective patches at the base of the accretionary complex. Micksch et al. (2006) reported reflectivity in the uppermost part of the plate interface above the subducting slab, also reflecting the subduction channel. In consequence, the subduction channel is hardly defined as the area in between the sharp reflector of the oceanic plate, and the highly reflective patches along the base of the upper plate. Additionally, the subduction channel is characterized as a low velocity zone in the area between the base of the upper plate and the top of the oceanic plate along the Chilean subduction zone (Krawczyk et al. 2006, and references therein).

In addition, Calvert (2004) mentioned two important reflectors at the northern Cascadia subduction zone. One reflector is referred to be the top of the downgoing plate, the other reflector is assumed to be the roof thrust of a duplex. The area in

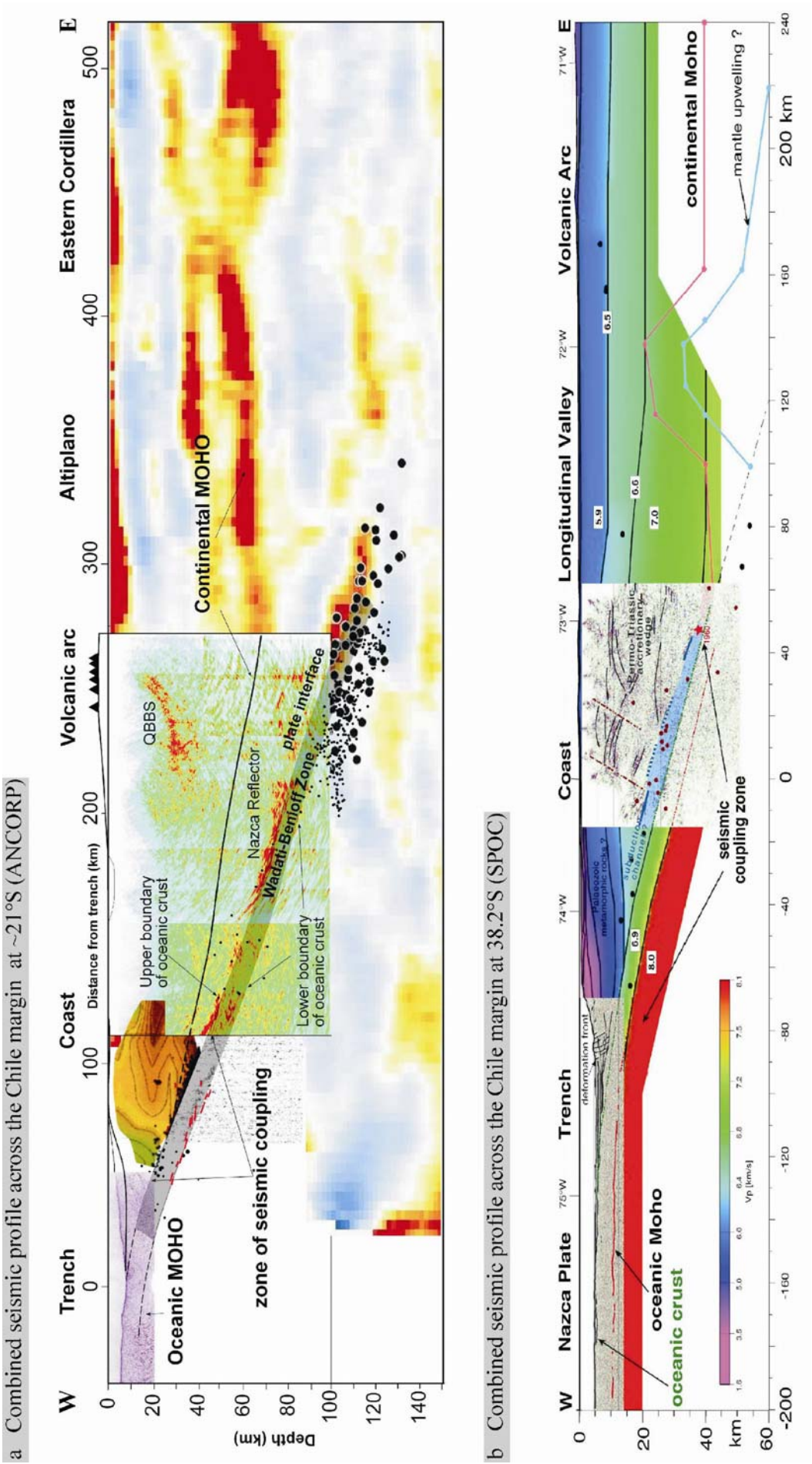
a Combined seismic profile across the Chile margin at ~21°S (ANCORP)
W
Trench
Coast
Volcanic arc
Altiplano
Eastern Cordillera
E
Distance from trench (km)
Depth (km)
Oceanic MOHO
zone of seismic coupling
Upper boundary of oceanic crust
Lower boundary of oceanic crust
QBBS
Nazca Reflector
Wadati-Benioff Zone
plate interface
Continental MOHO
b Combined seismic profile across the Chile margin at 38.2°S (SPOC)
W
Nazca Plate
Trench
Coast
Longitudinal Valley
Volcanic Arc
E
oceanic Moho
oceanic crust
seismic coupling zone
continental Moho
mantle upwelling ?
200 km
km

Figure 3.7: Seismic profiles crossing the Chile margin. a) Combined seismic profile crossing marine and onshore domains at about 21° S. Structural and tomographic data are shown to 150 km depth. QBBS: Quebrada Blanca Bright Spot. Data compilation after Krawczyk et al. 2006 and references therein. b) Combined seismic profile crossing marine and onshore domains at about 38.2° S. The wide-angle velocity model is overlain by structural and tomographic information and interpretation to 60 km depth. Data compilation after Krawczyk et al. 2006 and references therein.

between both reflectors is characterized by a V_P velocity of 6.8 km/s to 7.2 km/s, which is consistent with crustal rocks derived from both the oceanic and the lower continental plate. That gives an additional hint for the presence of a subduction channel transporting slivers from both the lower and the upper plate embedded within a sedimentary matrix towards depth.

The seismic velocity structure of convergent margins clearly highlights the subducting oceanic crust with a V_P of about 7 km/s, and the oceanic mantle with a V_P in the range of 8 km/s (Ito et al. 2000). The continental upper crust at 10 km to 15 km depth exhibits a V_P about 6.3 km/s, whereas the lower continental crust exhibits a V_P of 7.4 km/s, caused by the change from a felsic to a mafic composition. P-wave velocity of the continental mantle is assumed to achieve 8.0 km/s below 50 km depth and 8.34 km/s at approximately 90 km. Sediments exhibit lower velocities of about 2.0 km/s to 5.8 km/s at a depth range between <1 km and 5 km (Fig. 3.7). Subducted and accreted sediments should be responsible for the low P-wave velocities above the subducted oceanic plate (Husen et al. 2000). This zone of lower seismic velocities should delineate a possible subduction channel (see also Krawczyk et al 2006, and references therein). According to Husen et al. (2000), the base of the upper crust is marked by a strong V_P increase.

High V_P/V_S ratios are used as indicators for the presence of fluids (Husen et al. 2000) in the oceanic crust as well as along the plate interface. This points to possible fractures in the oceanic crust or the presence of water saturated sediments (Husen et al. 2000), respectively. The hydration or serpentinization of the fore-arc mantle wedge (Fig. 3.1) by fluids expulsed from the subducting slab is assumed to be responsible for V_P velocities of about 7.2 km/s to 7.3 km/s, which are too low for normal mantle rocks.